Cell, Vol. 120, 687–700, March 11, 2005, Copyright ©2005 by Elsevier Inc. DOI 10.1016/j.cell.2004.12.026

Arabidopsis Interdigitating Cell Growth Requires Two Antagonistic Pathways with Opposing Action on Cell Morphogenesis

Ying Fu,[1,3] Ying Gu,[1,3] Zhiliang Zheng,[1,4] Geoffrey Wasteneys,[2] and Zhenbiao Yang[1,*]
[1]Center for Plant Cell Biology
Institute for Integrative Genome Biology and
Department of Botany and Plant Sciences
University of California, Riverside
Riverside, California 92521
[2]Department of Botany
University of British Columbia
Vancouver
Canada

Summary

Coordinating growth and communication between adjacent cells is a critical yet poorly understood aspect of tissue development and organ morphogenesis. We report a Rho GTPase signaling network underlying the jigsaw puzzle appearance of *Arabidopsis* leaf pavement cells, in which localized outgrowth in one cell is coordinated with localized inhibition of outgrowth of the adjacent cell to form interdigitating lobes and indentations. Locally activated ROP2, a Rho-related GTPase from plants, activates RIC4 to promote the assembly of cortical actin microfilaments required for localized outgrowth. Meanwhile, ROP2 inactivates another target RIC1, whose activity promotes well-ordered cortical microtubules. RIC1-dependent microtubule organization not only locally inhibits outgrowth but in turn suppresses ROP2 activation in the indentation zones. Thus, outgrowth-promoting ROP2 and outgrowth-inhibiting RIC1 pathways antagonize each other. We propose that the counteractivity of these two pathways demarcates outgrowing and indenting cortical domains, coordinating a process that gives rise to interdigitations between adjacent pavement cells.

Introduction

Cell shape formation is important for the differentiation, behavior, and function of specific cells as well as for organ and tissue development and morphogenesis in multicellular organisms. Mechanisms underlying morphogenesis have been studied extensively in the unicellular yeast systems (Lew, 2003). Unlike unicellular systems, growth and morphogenesis within a developing organ require coordination between adjacent cells and are regulated by developmental and intercellular signals.

Interlocking jigsaw puzzle-shaped pavement cells in the leaf epidermis serve as an exciting model to investigate the mechanisms for cell shape formation in a multicellular system (Qiu et al., 2002; Deeks and Hussey, 2003; Smith, 2003; Wasteneys and Galway, 2003). The development of *Arabidopsis* leaf pavement cells is separated into three stages (Figure 1A) (Fu et al., 2002). Small and pentagonal or hexagonal initial cells expand preferentially along the leaf long axis to form slightly elongated polygons (stage I). The stage I cells initiate multiple outgrowths or localized lateral expansion from their anticlinal walls into adjacent cells, producing stage II cells with multiple shallow lobes alternating with indentations or necks. As early lobes expand, reiterative lobe and neck formation continues, resulting in highly lobed interlocking cells (stage III). This growth is presumably regulated by cell-to-cell signaling, allowing the spatiotemporal coordination of lobe outgrowth with inhibition of outgrowth and compensatory deformation in the corresponding indented region of the adjacent cell(s).

The cytoskeleton is implicated in the control of pavement cell development (Smith, 2003) (Figure 1A). Well-ordered cortical microtubule (MT) bundles arranged transversely in the neck regions are believed to restrict expansion in the direction of their predominant orientation (Wasteneys and Galway, 2003). In contrast, lobe initiation and outgrowth appear to require cortical fine actin microfilaments (MFs) localized to sites lacking well-ordered cortical MTs (Frank and Smith, 2002; Fu et al., 2002).

Organization of both cortical MFs and MTs is controlled by ROP GTPases, plant-specific members of the Rho GTPase family (Fu et al., 2002; Yang, 2002). Expression of a constitutively active *ROP2* mutant (*CA-rop2*) in *Arabidopsis* generates even distribution of the fine MFs throughout the cell cortex, delays formation of well-ordered cortical MTs associated with neck formation of stage II cells, and eliminates interdigitation by increasing expansion in the neck regions (Fu et al., 2002). A dominant-negative *ROP2* mutant (*DN-rop2*) inhibits lobe development by preventing fine MF formation. Rho family GTPases also play a pivotal role in morphogenesis in animal cells (Etienne-Manneville and Hall, 2002). Investigating the as yet unknown mechanisms of Rho GTPase signaling in leaf pavement cells may therefore provide a unifying mechanism for cell morphogenesis across plant and animal kingdoms.

In this report, we present evidence that pavement cell morphogenesis is controlled by the countersignaling of two ROP-mediated pathways with opposing effects on cell expansion. Locally activated ROPs promote lobe growth by activating RIC4-mediated assembly of fine cortical MFs as well as by inactivating RIC1-organized cortical MTs. The RIC1-MT pathway promotes neck formation and antagonizes the RIC4-actin pathway by repressing ROP activation. The countersignaling of these two pathways can explain the interdigitating separation of lobing and indenting domains of the cell cortex during the formation of interlocking pavement cells.

*Correspondence: zhenbiao.yang@ucr.edu
[3]These authors contributed equally to this work.
[4]Present address: Department of Biological Sciences, Lehman College, City University of New York, 250 Bedford Park Boulevard West, Bronx, New York 10468.

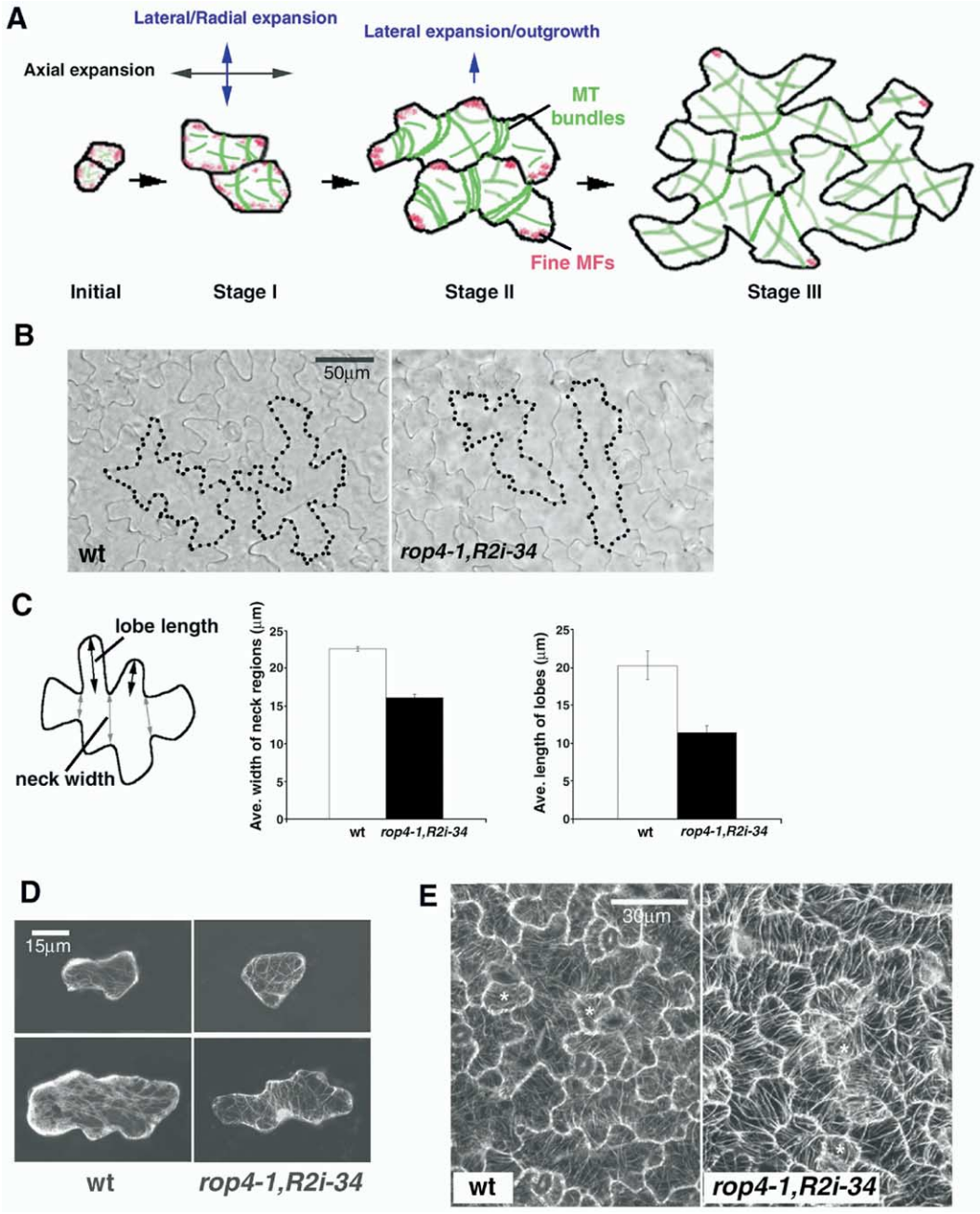

Figure 1. ROP GTPases Are Required for Localized Lateral Cell Expansion to Form Lobes and Modulate Cytoskeletal Organization

(A) A schematic illustration of *Arabidopsis* leaf pavement cell development and associated fine actin MTs (red patches) and MTs (green lines) in the cortex based on a previous description (Fu et al., 2002). ROP-independent actin bundles are not shown. Arrows indicate directions of expansion.

(B) Pavement cell shapes in the *rop4-1,R2i-34* line. The line was generated by transforming a *ROP2 RNAi* construct into the *rop4-1* knockout mutant (Figure S1).

(C) Quantitative analysis of *rop4-1,R2i-34* pavement cell shape changes. The carton on the left illustrates how the neck width and the lobe length were measured. The average neck widths and lobe lengths were significantly different ($p < 0.05$) between wt and the *rop4-1,R2i-34* line. All data are represented as mean ± standard deviation.

(D) Comparison of fine cortical MFs in stage I (top) and stage II (bottom) cells between wt and the *rop4-1,R2i-34* line. MFs were visualized using transiently expressed GFP-mTalin (Fu et al., 2002). Strong signals from fine cortical MFs were detected in 97% of stage I wt cells (n = 23) but only in 52% (n = 29) of *rop4-1,R2i-34* cells. In stage II, 88% of wt cells (n = 28) but only 31% (n = 26) of *rop4-1,R2i-34* cells contained detectable fine cortical MFs.

(E) Cortical MTs in late stage II cells from cauline leaves in wt and in the *rop4-1,R2i-34* line. MTs were visualized using stably expressed GTP-tubulin as previously described (Fu et al., 2002).

Results

ROP2 and ROP4 Control Pavement Cell Morphogenesis

We first determined that ROP2 and ROP4, which share 97% amino acid identity and are both expressed in leaves (Li et al., 1998), are functionally redundant in controlling pavement cell shape. A *rop4* knockout mutant (*rop4-1*) had only a weak cell shape phenotype, and a *ROP2* RNAi (*R2i*) line generated a slightly stronger but still moderate defect (see Figure S1 in the Supplemental Data available with this article online). Expressing *ROP2* RNAi (*R2i-34)* in the *rop4-1* mutant dramatically reduced neck expansion and lobe outgrowth (Figures 1B and 1C).

In the *rop4-1, R2i-34* line, the formation of fine cortical MFs, as visualized by transient expression of GFP-mTalin (Fu et al., 2002), was impaired. Fine cortical MFs were patchily localized to likely outgrowing regions of the cell cortex in wild-type (wt) pavement cells (Figure 1D) but were barely detectable in most *rop4-1,R2i-34* pavement cells, as seen in *DN-rop2* cells (Fu et al., 2002). Cytoplasmic MF bundles in the *rop4-1,R2i-34* cells were similar in appearance or more extensive and thicker than those in control cells, indicating that the elimination of fine cortical MFs in the mutant was not caused by lower *GFP-mTalin* expression levels. We conclude that ROP2 and ROP4 (ROP2/4) activities specifically promote the formation of fine cortical MFs.

To analyze the effect of ROP2/4 on cortical MTs, we crossed the *rop4-1,R2i-34* line to a *GFP-tubulin* line (Fu et al., 2002; Ueda et al., 1999). We compared cortical MTs between a control line (homozygous for *GFP-tubulin*) and a line homozygous for *GFP-tubulin*, *rop4-1*, *and R2i-34*. In stage I cells, the *rop4-1,R2i-34* line had more and thicker MT bundles than controls (data not shown). In stage II control cells, transversely ordered cortical MTs are only associated with the neck regions (Fu et al., 2002). In contrast, abundant and thick transverse cortical MTs were found throughout the whole length of stage II *rop4-1,R2i-34* cells (Figure 1E). Thus, ROP2/4 proteins suppress the formation of well-ordered cortical MT arrays in the early stages of pavement cell morphogenesis.

RIC1 Is Colocalized with Cortical MTs

Two possible mechanisms can explain the effects of loss of ROP2/4 function on both cortical MFs and MTs described above: (1) ROPs coordinately control two pathways respectively regulating MFs and MTs; and (2) a ROP pathway directly regulates one of the two cytoskeletal systems, which subsequently affects the other. To distinguish these possibilities, we sought to identify ROP2/4 target proteins. We previously identified a class of novel proteins as putative ROP targets from *Arabidopsis*, known as RICs (*R*OP-*i*nteractive *C*RIB motif-containing proteins (Wu et al., 2001). We transiently expressed *GFP-RICs* to survey the subcellular localization of those RICs expressed in leaves and found that GFP-RIC1 displayed cortical MT-like localization.

In young pavement cells, GFP-RIC1 was found at the plasma membrane (PM) as well as cortical structures resembling MTs (Figure 2A; Figure S2). By contrast, in older cells, GFP-RIC1 almost exclusively exhibited cortical MT-like localization, with strong GFP-RIC1 dots found along the filaments. This is reminiscent of the localization of some MT-associated proteins (MAPs) (Lloyd and Hussey, 2001). We confirmed RIC1's MT association in pavement cells using both live probes and immunolabeling strategies. Transiently expressed YFP-RIC1 colocalized with stably expressed GFP-tubulin, and MT depolymerization by oryzalin treatments abolished the filamentous pattern of YFP-RIC1 (Figure 2B). Double labeling cells with an anti-RIC1 antibody and anti-tubulin confirmed that native RIC1 is colocalized with cortical MTs in wt cells and is absent from *ric1-1* knockout cells (Figure 2C). Cosedimentation experiments demonstrated that RIC1 partially associates with MT polymers in vitro (Figure S2). Taken together, our results demonstrate that RIC1 is a novel MAP with a developmentally dependent distribution to both the PM and cortical MTs.

RIC1 Promotes MT Organization and Inhibits Lateral Expansion in the Neck Regions

To investigate whether RIC1 regulates cortical MT organization, we transiently coexpressed *RIC1* and *GFP-tubulin* in tobacco BY-2 cells. These experiments suggested that RIC1 promoted GFP-tubulin incorporation into well-ordered cortical MTs (Figure S3). To see if RIC1 promoted MT organization in *Arabidopsis* pavement cells, we generated *RIC1*-overexpressing lines (Figure 2D) and first tested how changing RIC1's expression affected cell morphology. Low-level *RIC1* overexpression (*RIC1 OX-11*) had no obvious effect on pavement cell shape (Figures 2E and 2G). As with the combined loss of ROP2 and ROP4 function (Figure 1E), moderate *RIC1* overexpression (*RIC1 OX-5*) inhibited lobe formation and reduced the width of the neck regions (Figures 2E and 2G). Higher levels of *RIC1* overexpression (*RIC1 OX-3*) completely suppressed lobe formation and generated elongated narrow cells with straight outlines (Figure 2G). These effects are distinct from those caused by *CA-rop2* mutants (Fu et al., 2002), which impair the formation of well-ordered MTs and generate wider than normal pavement cells with straight cell outlines (Figures 2F and 2G). Thus, RIC1 and ROP2/4 have an opposite effect on the spatial control of cell expansion, even though both affect the interdigitation process.

RIC1 overexpression also dramatically altered MT organization in pavement cells (Figure 2H). As early as stage I, cortical MTs in the *RIC1 OX-3* cells were more consistently transverse compared to those in wt cells and also appeared brighter, suggesting that RIC1 promotes MT bundling. In stage II *RIC1 OX-3* cells, the cell cortex was densely packed with parallel cortical MTs aligned perpendicular to the elongation axis. In contrast, such highly organized MTs were mainly present in the forming neck regions in wt stage II cells (Fu et al., 2002). Cortical MTs remained transverse and appeared to become more thickly bundled in stage III *RIC1 OX-3* cells, whereas stage III wt cells contain randomly oriented cortical MTs (Figure 2H). Transient *RIC1* overexpression in pavement cells rapidly induced apparent MT bundling and formation of well-ordered MTs

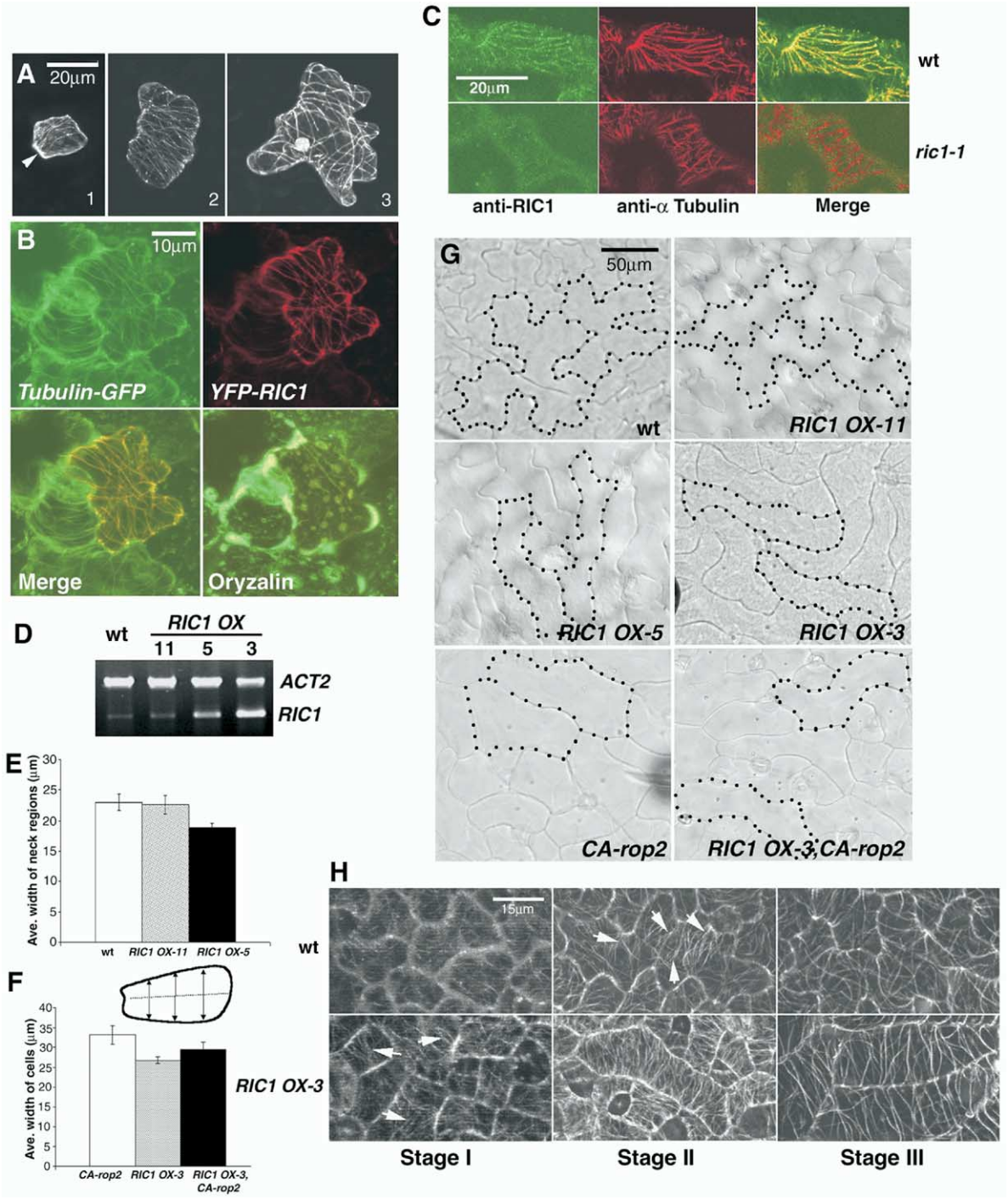

Figure 2. RIC1 Associates with and Promotes the Organization of Cortical MTs and Inhibits Lateral Cell Expansion

Images in (A), (B), (C), and (H) were projections from 10–20 μm serial confocal sections (0.8–1 μm per section).

(A) Transiently expressed GFP-RIC1 showed filamentous structures. Arrowhead indicates the RIC1 PM localization in a younger pavement cell.

(B) Colocalization of YFP-RIC1 (pseudocolor red) with cortical MTs (green). A *YFP-RIC1* construct was bombarded into pavement cells of the *GFP-tubulin* line. Merged image (lower left) shows an overlapping pattern (yellow) of YFP-RIC1 and GFP-tubulin. Treatment with 2 μM oryzalin (lower right) disrupted both MTs and YFP-RIC1 structures.

(C) Immunolocalization of native RIC1 in wt and *ric1-1* knockout mutant. Double staining of RIC1 and tubulin is described in text.

(D) RT-PCR analysis of RIC1 mRNA levels for RIC1-overexpressing lines (*RIC1OX-11*, *RIC1OX-5*, and *RIC1OX-3*) and wt (Col-0).

(E) Quantitative analysis of neck widths shows that *RIC1 OX-5* had significantly narrower necks than wt and *RIC1 OX-11*($p < 0.05$). All data are represented as mean ± standard deviation.

(F) Quantitative comparison of the average widths of pavement cells between the *RIC1 OX-3* line, a *CA-rop2* line, and a *RIC1 OX-3,CA-rop2* double homozygous line. The differences in cell widths among the three lines are significant ($p < 0.05$). All data are represented as mean ± standard deviation.

(G) Comparison of pavement cell shapes between the *RIC1*-overexpressing lines, the *CA-rop2* line, and the *RIC1 OX-3,CA-rop2* line.

(H) Increased organization of cortical MTs in *RIC1 OX-3* pavement cells. MTs were visualized with GFP-tubulin as described in (B). Arrows in the lower left panel indicate the well-ordered MTs in RIC1 OX-3 stage I cells, which were present in wt stage II cells.

before any detectable changes in cell shape (Figure S3). Thus, through its association with MTs and ability to induce changes in MT organization independent of cell shape change, RIC1 promotes the establishment of well-ordered cortical MTs.

We further explored RIC1 function by examining cell morphology and MT organization in *ric1-1 and ric1-2* knockout mutants. Neither mutant had detectable *RIC1* mRNA due to single T-DNA insertions in the third (*ric1-1*) and fourth (*ric1-2*) exons (Figure 3E). The two mutants had the same phenotype, and the *ric1-1* phenotype is described here. The wt phenotype was restored in *ric1-1* by expressing *RIC1* cDNA (Figure S4), demonstrating that the *ric1* phenotype was due to loss of RIC1 function. Although the cell shape change in *ric1-1* was not large (Figure 3A versus Figure 3B), neck regions were significantly wider compared to wt cells (Figure 3F). There was no significant difference in lobe length (Figure 3G). (Note that the *ric4-1* mutant and *ric4-1/ric1-1* double mutant are included in Figure 3 for comparison with *ric1* but will be described later.) Thus, the *ric1-1* phenotype is opposite to the *RIC1* overexpression phenotype and more similar to, though less severe than, the *CA-rop2* phenotype. Compared to wt, stage I *ric1-1* cells contained fewer and shorter cortical MTs and much more diffuse unincorporated GFP-tubulin (Figure 3H). In stage II *ric1-1* cells, cortical MTs were fewer, apparently less bundled, and not as uniformly oriented as in wt cells. We conclude that RIC1 promotes well-ordered MT arrays in the neck region, consequently restricting lateral expansion to generate the narrow neck morphology of pavement cells.

Activated ROP2 Suppresses RIC1 Function

The above observations show that ROP2/4 and RIC1 have opposite actions in both cortical MT organization and cell morphogenesis. RIC1 is known to interact with the GTP bound, active form of ROP1 in vitro (Wu et al., 2001). Thus, we postulated that activated ROP2/4 might bind to and inactivate RIC1. We used fluorescence resonance energy transfer (FRET) analysis as an initial test of this hypothesis. As shown in Figure 4A, strong FRET signals were detected in cells coexpressing CFP-RIC1 with YFP-CA-rop2 (active form) but not with YFP-DN-rop2 (inactive form), confirming RIC1's binding to the active but not the inactive form of ROPs. FRET signals in cells coexpressing CFP-RIC1 and YFP-CA-rop2 were primarily detected throughout the PM where CA-rop2 localizes (Fu et al., 2002). Furthermore, CFP-RIC1 was depleted from cortical MTs when coexpressed with YFP-CA-rop2, but remained associated with cortical MTs when coexpressed with YFP-DN-rop2 (Figure 4A).

These results suggest that PM-localized activated ROP2/4 may reduce RIC1's association with cortical MTs by sequestering RIC1. To test this possibility, we investigated how loss of ROP function and *CA-rop2* expression affected RIC1's distribution patterns. In wt cells at stage I, GFP-RIC1 was distributed between the PM and cortical MTs (Figure 4B); at stage II, GFP-RIC1 was mostly localized to cortical MTs, with some fluorescence at PM regions (Figure 4D). In *rop4-1,R2i-34* cells, the majority of GFP-RIC1 was localized to MTs at stage I (Figure 4C), and all GFP-RIC1 was distributed to MTs by stage II (Figure 4E). Furthermore, GFP-RIC1-decorated MTs were more numerous in the *rop4-1,R2i-34* line than in wt. GFP-RIC1 distribution in *DN-rop2* cells was similar to that in *rop4-1,R2i-34* cells (data not shown). Thus, loss of ROP2/4 activity increased RIC1's association with MTs.

In contrast, in stage I–II pavement cells, in which ROP2 activity was maintained at a constant level in *CA-rop2* transgenic plants (Fu et al., 2002), GFP-RIC1's association with MTs varied according to the level of transiently expressed GFP-RIC1 (Figures 4F–4H). When expression levels increased, as indicated by GFP fluorescence intensity, proportionately more of GFP-RIC1 became distributed to MTs. To further test whether activated ROP2 removes RIC1 from cortical MTs, we transiently coexpressed a fixed amount of *GFP-RIC1* with variable amounts of *CA-rop2*. Increasing amounts of *CA-rop2* caused more GFP-RIC1 to shift from cortical MTs to the PM; GFP-RIC1 was exclusively distributed at the PM in most cells transfected with the highest levels of *CA-rop2* tested (Figures 4I–4K; Figure S5). In addition, we crossed the *CA-rop2* line to the *RIC1 OX-3* line. *CA-rop2* expression partially suppressed the *RIC1* inhibition of lateral expansion (Figures 2F and 2G). Taken together, these results clearly indicate that activated ROP2 sequesters RIC1 and, by removing it from cortical MTs, inhibits the establishment of well-ordered cortical MTs.

Active ROP2 Interacts with RIC4 at Lobe Tips

Another ROP-interacting protein, RIC4, acts as a ROP1 target activating the assembly of apical MFs in pollen tubes (Fu et al., 2001; Y. Gu et al., submitted). *RIC4* is also expressed in leaves (Wu et al., 2001), so we investigated whether RIC4 might be a ROP2/4 target activating the assembly of fine MFs at cortical patches in pavement cells. We first examined RIC4 distribution using GFP-RIC4, which is functional as wt RIC4 in the control of pollen tube growth (Wu et al., 2001; Y. Gu et al., submitted). In contrast to the even cytoplasmic and nuclear distribution of GFP alone (Figure 5D), GFP-RIC4 was patchily distributed, primarily at the cell cortex, in a pattern suggestive of incipient lobes in stage I cells and to lobe tips in stage II cells (see arrows in Figures 5A and 5B). This localization pattern is dependent on ROP2/ROP4 activity, because it was eliminated in the *rop4-1,R2i-34* line (Figures 5E and 5F) and by transient overexpression of *DN-rop2* (data not shown). Finally, *CA-rop2* expression caused GFP-RIC4 to distribute evenly throughout the whole cell cortex (Figures 5C and 5C′).

FRET analysis also demonstrated that the RIC4 localization to potential incipient lobes and lobe tips may be the result of a direct interaction with activated ROP2/4. CFP-RIC4 strongly interacted with YFP-CA-rop2 in the cell cortex but not with YFP-DN-rop2 (Figure 5G). When wt ROP2 fused to YFP was used in the FRET assay, the CFP-RIC4/YFP-ROP2 FRET signal was patchily distributed in wt cells to presumed incipient lobes and lobe tips. Because RIC4 specifically interacts with active but not with inactive ROP2, these results strongly suggest that ROP2 is preferentially activated in the lobe-forming regions of the cell cortex.

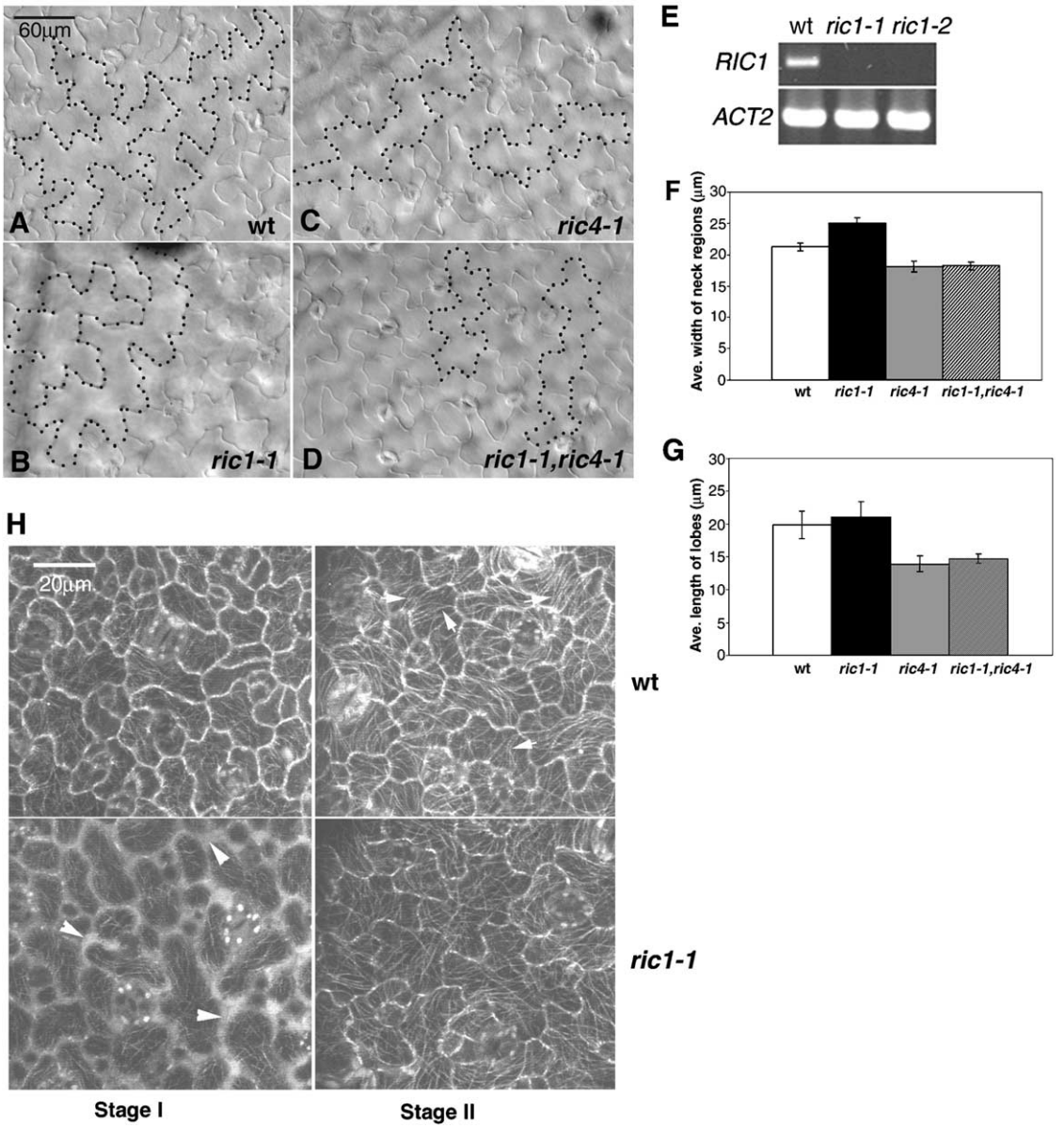

Figure 3. Phenotype Analysis of *ric1-1* Knockout Mutant in Comparison to *ric4-1* Knockdown Mutant and *ric1-1,ric4-1* Double Mutant

(A–D) Pavement cell shapes of wt (A), *ric1-1* (B), *ric4-1* (C), and *ric1-1,ric4-1* double mutants (D).

(E) RT-PCR analysis of *RIC1* transcript levels in *ric1-1* and *ric1-2* knockout mutants.

(F and G) Quantitative analysis of neck widths and lobe lengths for different *ric* mutants. The differences in neck widths (F) between wt and *ric1-1*, *ric4-1*, or the *ric1-1,ric4-1* line were significant ($p < 0.05$), but no significant differences were seen between *ric4-1* and *ric1-1,ric4-1* ($p > 0.05$). The average lobe lengths (G) were significantly different ($p < 0.05$) between wt and *ric4-1* or the *ric1-1,ric4-1* line but not between wt and *ric1-1* or between *ric4-1* and the *ric1-1,ric4-1* line. All data are represented as mean ± standard deviation.

(H) Comparison of cortical MTs, visualized using GFP-tubulin described in Figure 1, in pavement cells in *ric1-1* and wt. Arrowheads in the lower left panel indicate unincorporated GFP-tubulin in *ric1-1*; arrows in the upper right panel point to well-ordered MTs in wt stage II cells, which were rarely seen in *ric1-1*.

RIC4 Promotes the Assembly of Fine Cortical MFs and Lobe Development

To analyze RIC4 function, we first examined the effect of *RIC4* overexpression on MF organization. In the control, fine MFs were distributed throughout the cortex of early stage I cells and at incipient lobes and tips of expanding lobes in stage II cells (Figure 5H). *RIC4* overexpression increased accumulation and distribution of fine MFs in about 80% (n = 55) of both stage I and stage II cells but did not alter the organization of the cytoplasmic MF bundles (Figure 5H; Figure S7). In a *RIC4* knockdown mutant, *ric4-1*, which has reduced *RIC4* mRNA levels (Y. Gu et al., submitted), pavement cells exhibited both narrower necks and shallower lobes (Figures 3C, 3F, and 3G), similar to loss-of-function *rop* mutants. Furthermore, the accumulation of fine

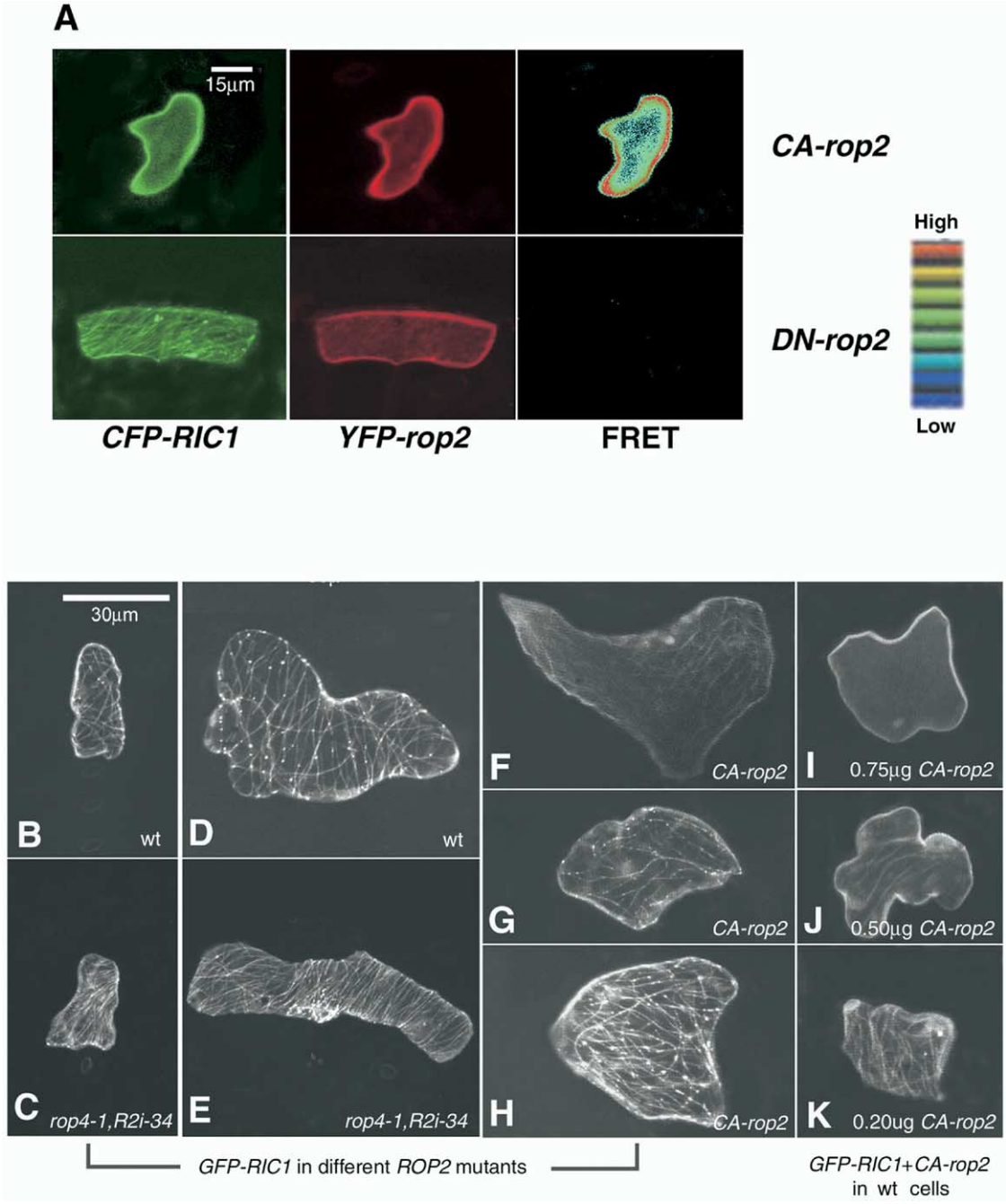

Figure 4. Activated ROP2 Binds RIC1 and Disrupts its Association with Cortical MTs

(A) In vivo interaction between RIC1 and a constitutively activated (CA-rop2) and dominant-negative form (DN-rop2) of ROP2 was studied using FRET analysis in pavement cells expressing *CFP-RIC1* and *YFP-CA-rop2* or *YFP-DN-rop2*. CFP (pseudocolored green) and YFP (pseudocolored red) signals were simultaneously collected,and the FRET signal was collected separately. The pseudocolor scale was used to indicate the FRET signal intensity.

(B–H) These panels show GFP-RIC1 localization in the pavement cells of wt (B and D), the *rop4-1,R2i-34* double (C and E), and the *CA-rop2* line (F–H). *GFP-RIC1* was transiently expressed.

(I–K) GFP-RIC1 localization in pavement cells transiently coexpressing a fixed amount of *GFP-RIC1* (1 μg *pBI221:GFP-RIC1*) with indicated amounts of *CA-rop2* (*pBI221:CA-rop2)*. All images shown were projections from 10–20 μm serial confocal sections (0.8–1 μm per section).

cortical MFs was greatly reduced in 79% (n = 43) of *ric4-1* cells (Figure 5H). *RIC4 (RNAi)*-induced suppression of *RIC4* expression caused similar phenotypes, confirming that the *ric4-1* mutation is responsible for the mutant phenotype (Figure S6). Finally, we confirmed genetically that RIC4 acts downstream of ROP2. The

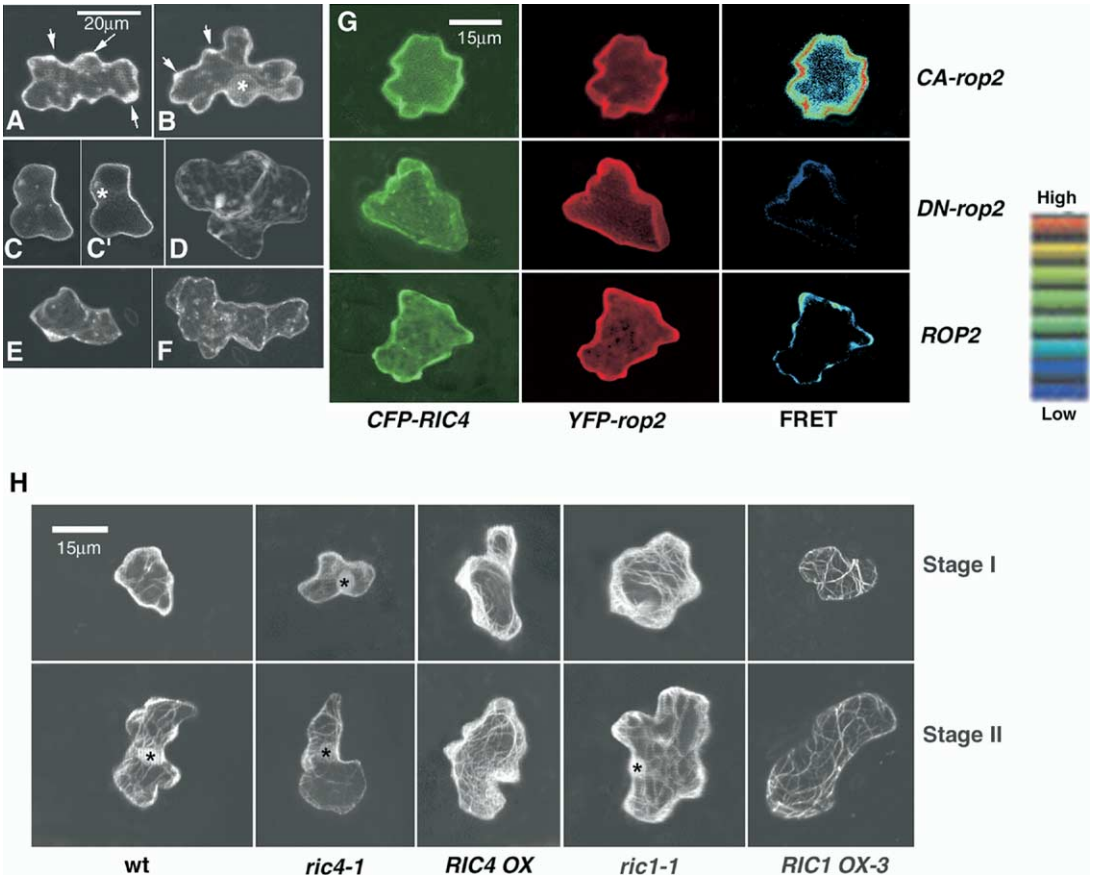

Figure 5. RIC4 Is a ROP2 Target Promoting the Assembly of Fine Cortical MFs

(A and B) Preferential distribution of GFP-RIC4 to incipient lobes and the tips of expanding lobes in wt pavement cells (arrows).

(C) *CA-rop2* expression caused GFP-RIC4 to disperse evenly throughout the cell periphery (PM). (C′) shows the midsection of the cell in (C). Asterisks indicate the position of the nucleus.

(D) Control cells expressing soluble GFP alone.

(E and F) Loss of GFP-RIC4 localization from lobe tips in the *rop4-1,R2i-34* line. Note slight increase in GFP-RIC4 in the cytoplasmic strands compared to (A) and (B).

(G) FRET analysis of RIC4 interaction with CA-rop2, DN-rop2, and wt ROP2.

(H) MF localization in different backgrounds. The *ric4-1*and *ric1-1* lines are described in Figure 3. *RIC1 OX* is the *RIC1 OX-3* line (Figure 2). *RIC4 OX* refers to transient overexpression of *RIC4* in wt background (0.5 μg DNA used). MFs were visualized using GFP-mTalin (see Figure 1). Asterisks indicate the nucleus.

ric4-1 mutation dramatically reduced the levels of fine cortical MFs generated by *CA-rop2* expression (Figure S7). Taken together, our results show that RIC4 is indeed a ROP2 target in leaf cells that promotes the assembly of fine cortical MFs required for lobe formation and lateral cell expansion.

RIC1 Suppresses the ROP2/RIC4 Promotion of Fine Cortical MFs

Since lobe expansion requires RIC4-dependent formation of fine cortical MFs, whereas *RIC1* overexpression suppresses lobe expansion, we postulated that RIC1 might inactivate the RIC4-dependent outgrowth-promoting pathway. We first examined ROP2/4- and RIC4-mediated fine cortical MFs in the *ric1-1* mutant and the *RIC1 OX-3* line. Indeed, the quantity of fine cortical MFs was dramatically increased in 83% (n = 23) of *ric1-1* stage I and II cells, but cortical MFs were absent in 90% (n = 44) of the *RIC1 OX-3* stage I and II cells (Figure 5H). If RIC1 acts upstream of RIC4 to inhibit the assembly of cortical MFs, we would expect *ric4-1* to be epistatic to *ric1-1*. Indeed, cell shape of the *ric1-1,ric4-1* double mutant is identical to that of *ric4-1* (Figures 3A–3G).

To investigate whether RIC1 suppressed the RIC4-dependent pathway by inactivating ROP2/4 signaling, we assessed the effect of *RIC1* expression on ROP2-RIC4 interaction using FRET analysis. Since RIC4 interacts with active but not inactive ROP2 (Figure 5), the strength of ROP2-RIC4 interaction reflects ROP2 activity. In wt stage II pavement cells, the RIC4-ROP2 FRET signals had a patchy distribution pattern, consistent with the apparent sites of lobe development (Figures 5 and 6). In the *ric1-1* stage II cells, the FRET signals were found throughout the cell cortex (Figure 6A). In contrast, in *RIC1 OX-3* cells, the FRET signals were barely detectable anywhere. Semiquantitative analysis shows that the *ric1-1* mutation and *RIC1* overexpression

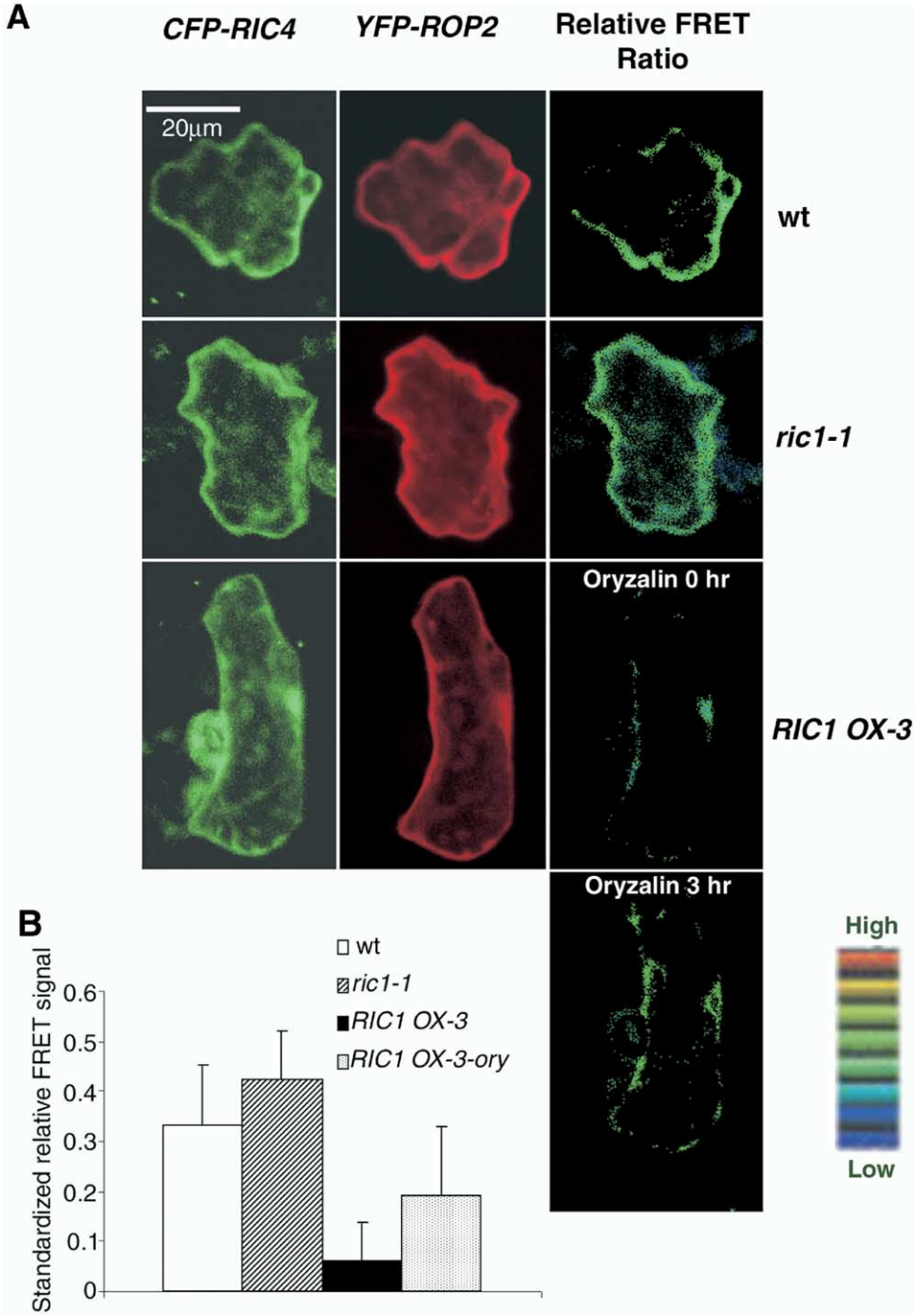

Figure 6. RIC1 and Cortical MTs Suppress ROP2 Interaction with RIC4

FRET analysis of the interaction between wt ROP2 and RIC4 in pavement cells was performed in *ric1-1*, *RIC1 OX-3*, or *RIC1 OX-3* cells treated with oryzalin (2 μM) for 0 or 3 hr.

(A) Representative images of the FRET signals.

(B) Semiquantitative analysis of FRET signals. The average signal per cell was significantly higher ($p < 0.05$) in *ric1-1* cells (n = 15) but dramatically lower in *RIC1 OX-3* cells (n = 15) compared to wt cells (n = 15). Treatment of *RIC1 OX-3* cells (n = 15) with oryzalin for 3 hr significantly increased the FRET signal ($p < 0.05$). All data are represented as mean ± standard deviation.

clearly had an opposite effect on the overall amount of the ROP2-RIC4 interaction (Figure 6B). These results demonstrate that RIC1 can inhibit ROP2-RIC4 interaction in a spatially controlled manner.

MT Polymer Status Regulates ROP2-RIC4 Interaction

RIC1suppression of the ROP2-RIC4 interaction could be regulated through a direct competition between

RIC1 and RIC4 for active ROP2, in which case MT disassembly would favor RIC1 release and the suppression of ROP2-RIC4 interaction. Alternatively, ROP2 activity could be regulated by some other MT-associated element(s), whose release from MTs may be regulated through RIC1's promotion of cortical MT assembly. To distinguish these possibilities, we performed FRET analysis of ROP2-RIC4 interaction after depolymerizing MTs. For this, the *RIC1OX-3* line, in which ROP2-RIC4 FRET signals are normally not detected, was treated with the MT destabilizing drug oryzalin. After 3 hr, MT polymers in *RIC1OX-3* cells were severely disrupted, and FRET signals were significantly increased (Figure 6). Longer treatment (7 hr) further increased the ROP2-RIC4 FRET signal (data not shown). The treatments also caused a dramatic increase in the quantity of fine cortical MFs, both in wt and *RIC1OX-3* cells (Figure S8), consistent with a role for cortical MTs in suppressing the ROP2-RIC4 pathway. We further tested the effect of disrupting cortical MTs on ROP2-RIC4 interaction using a temperature-sensitive *mor1* mutant. These mutants were isolated in a screen for aberrant MT organization in pavement cells (Whittington et al., 2001) that identified MOR1 as a member of the XMAP215 family of MAPs. At the restrictive temperature, *mor1-1* pavement cells showed severe fragmentation of cortical MT arrays and significantly increased ROP2-RIC4 FRET signals, whereas neither MT organization nor ROP2-RIC4 interaction was affected in wt cells at *mor1-1*'s restrictive temperature (Figure S9). This effect was reversible when *mor1-1* plants were returned to the permissive temperature, demonstrating that it is the status of MT polymers that regulates ROP2-RIC4 interaction in pavement cells.

By disassembling MTs by two different RIC1-independent mechanisms, we found that ROP-RIC4 interaction was enhanced. Thus, MT depolymerization is unlikely to significantly increase the amount of RIC1 available to compete with RIC4 binding to active ROP. This indicates that a MT-associated element other than RIC1 can stimulate ROP2 activation and that its sequestration by MTs is controlled by RIC1-mediated MT assembly. Collectively, our data indicate that RIC1 antagonizes the ROP2/RIC4-dependent pathway at least in part through its promotion of cortical MT organization.

Discussion

Our findings have several significant implications. Our work reveals a Rho GTPase signaling network underpinning interdigitation cell growth in a developing tissue that requires cell-cell coordination and communication. Furthermore, our data identify the first signaling pathway to control cortical MT organization as well as the first mechanism underscoring crosstalk between MTs and MFs in plant cells. In addition, our work demonstrates the conservation of Rho GTPase coordination of MFs and MT in plants, unifying the underlying mechanism for cell morphogenesis across animal and plant kingdoms (Kodama et al., 2004). This is particularly intriguing given the fundamental differences in physical requirements for shape formation between plant and animal cells.

Interdigitating Growth Is Controlled by a Rho GTPase Signaling Network with Two Counteracting Pathways

Our current data support a model of a Rho GTPase signaling network that controls interdigitating growth during pavement cell development (Figure 7). The network has at least two counteracting pathways that separately coordinate the formation of lobes and indentations. To form lobes, localized ROP activity turns on the RIC4 pathway, which promotes the assembly of fine cortical MFs necessary for localized wall loosening and bulge formation. The same ROP activity locally suppresses the RIC1 pathway. When active, however, RIC1 promotes well-ordered cortical MT arrays in other regions of the cell, and the RIC1-MT pathway in turn represses the ROP-RIC4-actin pathway. Well-organized cortical MT arrays constrain lateral or radial expansion to generate the indentations of pavement cells. Countersignaling between the ROP-RIC4-actin pathway and the RIC1-MT pathway can thereby establish cell surface demarcations that separate lobe-forming from indentation-forming domains. The formation of these demarcations within one cell may influence complementary demarcations in adjacent cells, allowing the coordination between neighbors to form highly lobed and interlocking cells.

Lobing Requires ROP/RIC4-Mediated MF-Based Localized Outgrowth

Loss-of-function and gain-of-function analyses show that active ROP2/ROP4 is required and sufficient for localized cell growth to form lobed pavement cells (Fu et al., 2002; this study). ROPs 2 and 4 promote localized cell outgrowth at least in part by activating RIC4 to promote assembly of cortical MFs. First, GFP-RIC4 was predominantly distributed in forming lobe tips in a ROP2/4-dependent manner. Second, RIC4 interacted with the active but not inactive form of ROP2. Third, *RIC4* overexpression and *CA-rop2* expression both generate fine cortical MFs throughout the cell cortex, whereas loss-of-function mutations for *RIC4* as well as *ROP2/4* can prevent cortical MF formation. Fourth, *CA-rop2* induction of fine cortical MFs is RIC4 dependent. The function of RIC4 in pavement cells is thus similar to its role as a ROP1 target promoting the assembly of apical actin networks during tip growth in pollen tubes (Y. Gu et al., submitted).

An interesting question is how RIC4 regulates MF assembly, since RIC4 is a novel protein with no homology to known Rho effectors for actin polymerization, e.g., N-WASP. RIC4 might promote actin assembly through a novel mechanism but could also link ROPs to the Arp2/3 complex through the WAVE/HSPC300 complex, as mutations in homologs for subunits of these complexes cause partial defects in the lobing of pavement cells (Deeks and Hussey, 2003; Frank and Smith, 2002; Le et al., 2003; Li et al., 2003; Mathur et al., 2003).

RIC1-Organized Cortical MTs Contribute to Neck Formation by Locally Constraining Outgrowth

We have demonstrated an important role for RIC1-dependent organization of cortical MTs in the local restriction of lateral expansion, generating the RIC1-

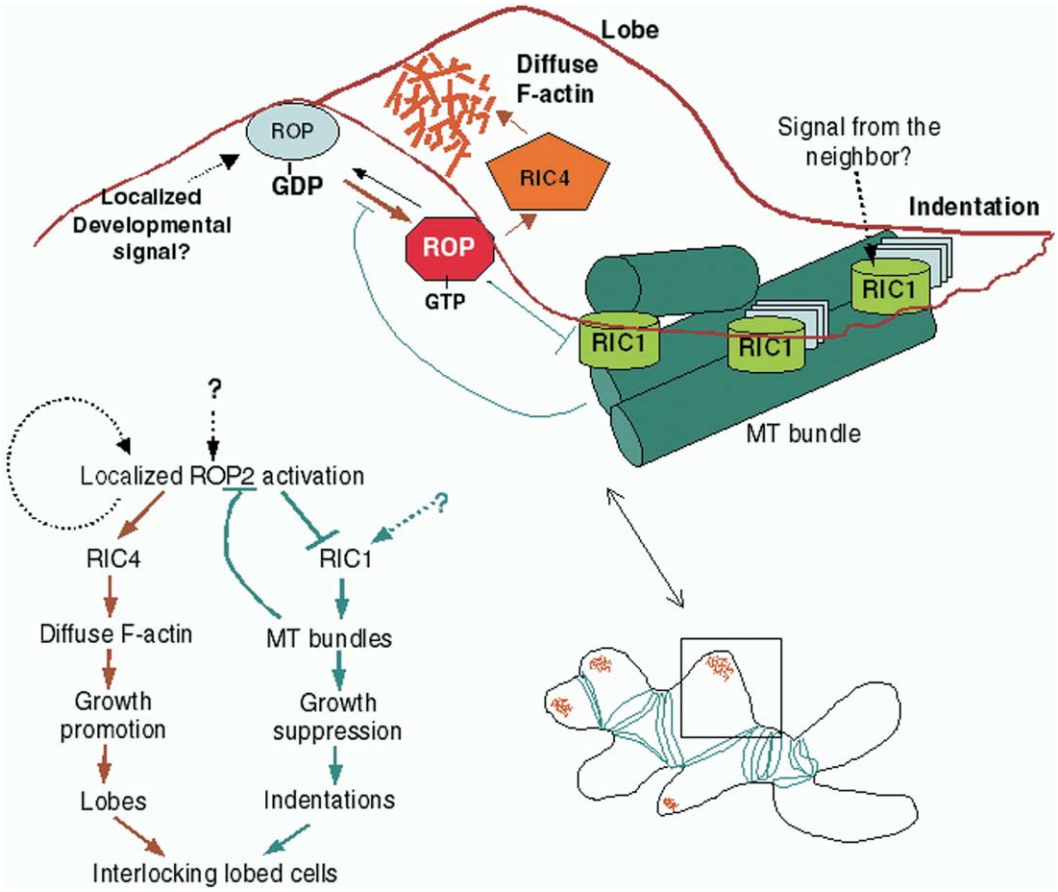

Figure 7. A Model for ROP GTPase Control of Pavement Cell Morphogenesis

Interdigitating growth in *Arabidopsis* leaf pavement cells is controlled by a ROP GTPase signaling network containing two counteracting pathways with opposing actions on localized cell expansion: the ROP-RIC4 pathway promotes lobe outgrowth via a fine cortical MF network, while the RIC1 pathway suppresses outgrowth via well-organized cortical MTs. We postulate that, during the initiation of lobes and indentations, these two pathways are locally activated and spatially separated, but they may subsequently counteract each other as a result of their respective self-amplification along the cell cortex. The countersignaling establishes borders that separate outgrowth-promoting from outgrowth-suppressing domains of the cell cortex. Solid arrows indicate steps supported by direct experimental evidence, and dotted arrows show hypothetical steps with some direct evidence.

dependent narrow neck morphology. RIC1 directly associates with and promotes the formation of well-ordered cortical MTs. Overexpressing *RIC1* promotes apparent bundling and transverse alignment of cortical MTs, whereas knocking it out has an opposite effect. RIC1's mode of action requires further investigation, but it induces parallel MT organization either by promoting MT polymerization or stabilization and/or directly activating MT bundling. A RIC1-independent mechanism also contributes to MT organization, as some cortical MTs are present in the *ric1-1* knockout pavement cells, especially during the later stages.

Spatial Separation of RIC1 and RIC4

Due to the respective roles for the ROP/RIC4 and the RIC1 pathways in lobe outgrowth and neck formation, we anticipate that these two pathways are localized in the corresponding regions of the cell cortex. Indeed, both ROP2 and RIC4 are preferentially localized to the tips of growing lobes (Figure 5) (Fu et al., 2002), and our FRET analysis of ROP-RIC4 interaction suggests that ROP2 is activated in incipient lobes and at the tips of growing lobes. Wt ROP2 and RIC4 is dispersed uniformly to the PM in *CA-rop2* cells but is shifted to the cytosol in *DN-rop2* cells (Fu et al., 2002) (Figure 5), supporting a positive feedback regulation of ROP signaling that allows ROP activity to self-amplify laterally.

Our observations also support the notion that RIC1 activity is localized in the indentation-forming regions and that, like ROP2/RIC4, it can be amplified laterally. In these neck regions, RIC1 is associated with transversely oriented, probably bundled arrays of cortical MTs. Knocking out *RIC1* specifically increases neck widths, suggesting that the functional activity of RIC1 is restricted to the neck region in wt pavement cells. However, moderate *RIC1* overexpression reduces the neck width and also partially inhibits lobe expansion, while high levels of overexpression completely inhibit lobe formation, suggesting that RIC1 activity can spread laterally from the neck to the lobe if overpro-

duced. Through local suppression of ROP activity (see below for further discussion), highly bundled MT polymers will reinforce RIC1 activity, in turn promoting further assembly and stabilization of cortical MTs, and thus could self-amplify laterally.

Counterregulation of the Two Pathways with Opposing Actions on Cell Expansion in Morphogenesis

Given the self-amplification of both the lobe-promoting ROP-RIC4-actin pathway and the neck-promoting RIC1-MT pathway along the cell cortex, these two pathways must counteract each other to establish borders separating the lobe-forming from the indentation-forming activity. Under this scenario, activated ROP2 coordinates RIC4 activation with RIC1 inactivation, resulting in lobe formation. ROP2 inactivation of RIC1 can explain the absence of cortical MTs in lobe tips. In contrast, suppression of the outgrowth-promoting ROP-RIC4 pathway by the RIC1-MT pathway assures the formation of narrow necks and explains the absence of fine cortical MFs in the neck regions.

How does ROP2/4 activity inactivate the RIC1-MT pathway? Our data confirm a direct interaction between RIC1 and activated ROP2 at the PM. Loss-of-function *rop2* and *rop4* mutations and *DN-rop2* expression all increase RIC1's association with cortical MTs, suggesting that ROP activity negatively regulates RIC1-MT interaction. This was confirmed by expressing CA-ROP2, which apparently sequestered RIC1 away from MTs (Figure 4), delaying the formation of well-ordered cortical MTs (Fu et al., 2002). This sequestration mechanism helps explain the changing distribution of RIC1 seen over the course of pavement cell development in wt plants, i.e., shifting from the PM (where active ROP2 is localized) to cortical MTs as ROP2/4 activity is expected to be downregulated in the later stages of the development. Finally, consistent with the effect of *CA-rop2* on RIC1 localization, *CA-rop2* expression partially counteracted the *RIC1* overexpression-induced inhibition of lateral cell expansion.

Our data also demonstrate that the RIC1-MT pathway inhibits the ROP2 activation of RIC4. *RIC1* overexpression reduced ROP2-RIC4 interaction, whereas knocking out *RIC1* expression enhanced ROP2-RIC4 interaction and generated a fine actin network throughout the cell periphery (Figure 6). Moreover, the *ric1-1* knockout mutation did not alter the *ric4* knockdown phenotype, consistent with RIC1 acting upstream of RIC4 through ROP2 inactivation. Finally, we determined that RIC1's negative regulation of the ROP2/4-RIC4 lobe-forming pathway is dependent on RIC1's promotion of MT polymerization.

The countersignaling mechanism may have much broader implications for the regulation of cell expansion in most plant cells whose geometry is less complex than that in pavement cells. It is generally noted that, in diffusely expanding cells of elongating organs, MT and MF distribution patterns at the nonexpanding end walls and rapidly expanding lateral walls show considerable differences (Wasteneys and Galway, 2003). Recent experiments have demonstrated that cortical MTs regulate the anisotropic properties of cell walls by some mechanism other than through the orientation of load-bearing cellulose microfibrils (Himmelspach et al., 2003). MT-dependent suppression of ROP signaling could be a key component of MT-dependent anisotropic cell expansion.

Rho GTPase Coordination of Actin and MTs: A Common Theme across Eukaryotic Kingdoms

In conclusion, ROP modulation of cortical MFs and MTs expands the emerging theme of Rho family GTPase coordination of MFs and MTs found in animal cells (Etienne-Manneville and Hall, 2002; Kodama et al., 2004). This unifying theme is extended to the ability of the cytoskeleton to provide signals for feedback regulation of Rho GTPases. Here we have shown that cortical MT organization negatively regulates ROP activity. In animal systems, MT polymerization has been implicated in both positive and negative regulation of Rho GTPase activation (Kodama et al., 2004; Franz and Ridley, 2003).

Behind this general theme lie molecular and mechanical differences that can explain why Rho GTPases coordinate MF and MT organization in such diverse biological systems. In animal cells, exploratory MT ends and pushing fine F-actin branches coordinate with each other to define polarity at the leading edge. Thus, Cdc42/Rac GTPases in animal cells can positively regulate the polymerization and stabilization of both F-actin and MTs using the same effector protein (Cau et al., 2001). In contrast, cortical F-actin and MTs have distinct roles in the regulation of cell expansion in plants. Accordingly, ROPs activate the assembly of fine cortical MFs but inhibit the assembly and organization of cortical MTs through two distinct target proteins, RIC4 and RIC1, respectively. ROP GTPase inhibition of MT organization is a departure from Rho family GTPase promotion of MT end capturing, polymerization, and stabilization in animal cells (Cau et al., 2001; Fukata et al., 2002; Wittmann et al., 2003).

Experimental Procedures

Plant Materials and Growth Conditions

A. thaliana ecotypes Col-0 and WS were used in this study. Transgenic plants expressing *CA-rop2* and *DN-rop2* mutant genes were described previously (Li et al., 2001). The *GFP-α-tubulin* transgenic line was kindly provided by Dr. T. Hashimoto (Ueda et al., 1999). Plants were grown at 22°C in soil with 16 hr light/8 hr dark cycles unless indicated otherwise.

Plasmid Construction

Plasmids used for transient expression were constructed in *pBI221* (Clontech, Palo Alto, CA). *pBI221:GFP-mTalin* and *pBI221:CA-rop2* were as described (Fu et al., 2002). *RIC1* and *RIC4* coding sequences (Wu et al., 2001) were amplified and cloned into the BamHI and SacI sites of *pBI221* to generate *pBI221:RIC1* and *pBI221:RIC4*. The same *RIC1* and *RIC4* cDNAs were subcloned into *pBI221:GFP* (Fu et al., 2002) to generate *pBI221:GFP-RIC1* and *pBI221:GFP-RIC4*. For colocalization or FRET experiments, GFP from the above constructs was replaced with CFP. For YFP constructs, we used *pBS35S:YFP* provided by Dr. A. von Arnim. *RIC1* was cloned into the BglII and SacI sites of *pBS35S:YFP. ROP2* was cloned into the BglII and BamH1 sites of *pBS35S:YFP. 35S:YFP* fragment replaced *35S:GFP* in *pBI221:GFP-CA-rop2* and *GFP-DN-rop2*, generating*pBI221:YFP-CA-rop2* and *pBI221:YFP-DN-rop2.*

Generation of *Arabidopsis RIC1* Overexpressing and Knockout Lines

To produce *RIC1* overexpressing lines, *35S:RIC1* was cut from *pBI221:RIC1* and cloned into *pCambia3300* (*pC3300*) to generate *pC3300:RIC1*. The construct was introduced into *A. thaliana* ecotype Col-0 using *Agrobacterium*-mediated transformation (Clough and Bent, 1998). BASTA-resistant transgenic plants were selected, and homozygous lines were identified.

We screened *RIC1* T-DNA insertion mutants from the Wisconsin's BASTA collection (Weigel et al., 2000). PCR and DNA gel blot analyses were performed to identify pools containing T-DNA insertions in *RIC* genes. Seeds for positive pools were obtained from the *Arabidopsis* Biological Resource Center (Columbus, OH), and single homozygous T-DNA insertion lines were identified from the pools by PCR analysis.

Light Microscopy Analysis of Leaf Pavement Cell Shapes

The third true leaf (0.6–0.8 cm in length and 0.4–0.5 cm in width) from 2-week-old seedlings was used for phenotype analysis as described (Fu et al., 2002). The width of neck regions and the length of lobes were measured as illustrated in the legend of Figure 1C. The measurements were consistently conducted on cells located in the midregion of the leaves of the same developmental stage. Each data set was from the measurement of at least 300 cells collected from three different leaves from three individual plants. For each leaf, four photos, each including at least 30 cells, were consistently taken in the midregion of the leaf. Consequently, the data were extremely reproducible.

Ballistics-Mediated Transient Expression in Leaf Epidermal Cells

All plasmids were purified as described (Fu et al., 2002). Routinely, 0.8 μg of *pBI221:GFP-mTalin*, *pBI221:GFP-α-tubulin*, *pBI221:GFP-RIC1* (or *pBI221:YFP-RIC1*), *pBI221:GFP-RIC4* constructs were used. For FRET analysis, 1.0 μg *pBI221:CFP-RIC1* or *pBI221:CFP-RIC4* and 0.65 μg *pBS35:YFP-ROP2* or *pBI221:YFP-CA-rop2/DN-rop2* constructs were used. For coexpression, 0.8 μg *pBI221:GFP-RIC1* or *pBI221:GFP-RIC4* with 0.5 μg *pBI221:CA-rop2* were routinely used unless otherwise indicated. The particle bombardment procedure was described previously (Fu et al., 2002).

Confocal Microscopy

MFs were visualized using transiently expressed GFP-mTalin as described (Fu et al., 2002). To visualize MTs in different mutant lines, they were crossed to the *tubulin-GFP* line (Ueda et al., 1999), and progenies homozygous for both the mutant gene and tubulin-GFP were analyzed using a Bio-Rad MRC-600 confocal laser scanning device as described previously (Fu et al., 2002).

Colocalization of YFP and CFP (or GFP) was performed using the Leica TCS SP2 confocal microscope, which allows flexible selection of emission bandwidths to minimize bleach-through. To colocalize MTs and RIC1, pavement cells in the tubulin-GFP line were transformed with *YFP-RIC1* by the ballistics method (Fu et al., 2002). Transformed cells were excited with 488 nm laser (power 20%) and 514 nm laser (50% power), and GFP and YFP signals were collected using 495–510 nm and 560–640 nm bandwidths, respectively. This setting did not completely eliminate the bleach-through of GFP signals to the YFP channel. However, any bleach-through signal was removed by adjusting the gain in the YFP channel against the tubulin-GFP background signal in neighboring nontransformed cells. For colocalization of CFP and YFP, 442 nm laser (power 15%) and 514 nm laser (power 15%) were used for excitation. CFP and YFP signals were collected using 465–490 nm and 560–640 nm bandwidths, respectively. For 3D reconstruction, optical sections were taken for each cell at 0.5–1.0 μm increments using the Leica software. Additional image analysis and processing were performed by MetaMorph 4.5 and Adobe Photoshop 5.5.

FRET Analysis

For FRET analysis, *pBI221:CFP-RIC1* or *-RIC4* was transiently coexpressed with *pBS35S:YFP-ROP2*, pBI221:YFP*CA-rop2*, or *-DN-rop2* in pavement cells. FRET analysis was performed 4–6 hr after particle bombardment unless otherwise indicated. Since expression levels for a specific pair of constructs varied among individual cells examined, over-/underflow function was applied to adjust the proper gain of CFP channel for each cell to avoid a saturating signal. Those cells in which the proper gain was found between 520 and 620 units (arbitrary units) were chosen to perform the FRET analysis. CFP (465–490 nm) and YFP (560–640 nm) images were simultaneously acquired prior to the acquisition of FRET images at the same focal plane to show the RIC4 and ROP2 localizations. FRET signals were consistently acquired using 15% power of the 442 nm laser for excitation and 560–640 nm for emission. The gain of the FRET channel was set 30 units lower than the CFP channel, which was based on the control experiments as described below. This setting sacrificed some FRET signals but effectively eliminated any bleach-through signals.

To further confirm that the FRET signals were not due to bleach-through, we performed a large number of control experiments using *pBI221:CFP-RIC1* or *-RIC4* and *pBS35S:YFP* pairs. We found all cells (at least 15 cells for each control) that expressed CFP-RIC and YFP to the levels that fell into the above range and did not show any detectable signals using the setting as described above. For semiquantitative analysis of FRET signals, we standardized FRET signals with CFP signals, which were acquired simultaneously. This standardization obviates FRET signal variation resulting from different CFP expression levels among different cells.

RIC1 Immunolocalization

RIC1 fusion protein (to maltose binding protein, MBP) expressed in *E. coli* was purified and used to raise polyclonal antibodies in rabbits. The RIC1 polyclonal antibody was affinity purified using the recombinant MBP-RIC1 protein as described (Lin and Yang, 1997). This antibody specifically detected signals along cortical MTs in wt but not in *ric1-1* cells (Figure 3C).

Immunostaining followed the procedure previously described (Wasteneys et al., 1997). Briefly, true leaves from 2-week-old plants were cut into 2 × 2 mm pieces, fixed, frozen, shattered, and permeabilized (Wasteneys et al., 1997). The fixed tissues were incubated with the primary antibodies (anti-RIC1, 1:100; mouse anti-α tubulin, 1:300, Sigma) and then the secondary antibodies (FITC-conjugated anti-rabbit IgG and TRITC-conjugated anti-mouse IgG, 1:200, Sigma). The samples were analyzed using the Leica SP2 confocal microscope system.

Supplemental Data

Supplemental data include nine figures, text, and Supplemental References and can be found with this article online at http://www.cell.com/cgi/content/full/120/5/687/DC1/.

Acknowledgments

We thank Bo Liu, Sidney Shaw, and Andre Jagendorf for their critical comments on the manuscript; the Salk Institute Genomic Analysis Laboratory for providing the sequence-indexed *Arabidopsis* T-DNA insertion mutants; John Fowler for providing *pBS-CFP* vector; and Albrecht Arnim for *pBS35S:YFP* vector. This work is supported by NSF grant (IBN-0417255) to Z.Y.

Received: January 28, 2004
Revised: December 1, 2004
Accepted: December 21, 2004
Published: March 10, 2005

References

Cau, J., Faure, S., Comps, M., Delsert, C., and Morin, N. (2001). A novel p21-activated kinase binds the actin and microtubule networks and induces microtubule stabilization. J. Cell Biol. *155*, 1029–1042.

Clough, S.J., and Bent, A.F. (1998). Floral dip: a simplified method for Agrobacterium-mediated transformation of *Arabidopsis thaliana*. Plant J. *16*, 735–743.

Deeks, M.J., and Hussey, P.J. (2003). Arp2/3 and 'the shape of things to come'. Curr. Opin. Plant Biol. *6*, 561–567.

Etienne-Manneville, S., and Hall, A. (2002). Rho GTPases in cell biology. Nature *420*, 629–635.

Frank, M.J., and Smith, L.G. (2002). A small, novel protein highly conserved in plants and animals promotes the polarized growth and division of maize leaf epidermal cells. Curr. Biol. *12*, 849–853.

Franz, C.M., and Ridley, A.J. (2003). p120ctn associates with microtubules: inverse relationship between microtubule binding and Rho GTPase regulation. J. Biol. Chem. *279*, 6588–6594.

Fu, Y., Wu, G., and Yang, Z. (2001). Rop GTPase-dependent dynamics of tip-localized F-actin controls tip growth in pollen tubes. J. Cell Biol. *152*, 1019–1032.

Fu, Y., Li, H., Yang, Z., Jones, M.A., Shen, J.J., and Grierson, C.S. (2002). The ROP2 GTPase controls the formation of cortical fine F-actin and the early phase of directional cell expansion during *Arabidopsis* organogenesis. Plant Cell *14*, 777–794.

Fukata, M., Watanabe, T., Noritake, J., Nakagawa, M., Yamaga, M., Kuroda, S., Matsuura, Y., Iwamatsu, A., Perez, F., and Kaibuchi, K. (2002). Rac1 and Cdc42 capture microtubules through IQGAP1 and CLIP-170. Cell *109*, 873–885.

Himmelspach, R., Williamson, R.E., and Wasteneys, G.O. (2003). Cellulose microfibril alignment recovers from DCB-induced disruption despite microtubule disorganization. Plant J. *36*, 565–575.

Kodama, A., Lechler, T., and Fuchs, E. (2004). Coordinating cytoskeletal tracks to polarize cellular movements. J. Cell Biol. *167*, 203–207.

Le, J., El-Assal Sel, D., Basu, D., Saad, M.E., and Szymanski, D.B. (2003). Requirements for *Arabidopsis* ATARP2 and ATARP3 during epidermal development. Curr. Biol. *13*, 1341–1347.

Lew, D.J. (2003). The morphogenesis checkpoint: how yeast cells watch their figures. Curr. Opin. Cell Biol. *15*, 648–653.

Li, H., Wu, G., Ware, D., Davis, K.R., and Yang, Z. (1998). *Arabidopsis* Rho-related GTPases: differential gene expression in pollen and polar localization in fission yeast. Plant Physiol. *118*, 407–417.

Li, H., Shen, J., Zheng, Z., Lin, Y., and Yang, Z. (2001). The Rop GTPase switch controls multiple developmental processes in *Arabidopsis*. Plant Physiol. *126*, 670–684.

Li, S., Blanchoin, L., Yang, Z., and Lord, E.M. (2003). The putative *Arabidopsis* arp2/3 complex controls leaf cell morphogenesis. Plant Physiol. *132*, 2034–2044.

Lin, Y., and Yang, Z. (1997). Inhibition of pollen tube elongation by microinjected anti-Rop1Ps antibodies suggests a crucial role for Rho-type GTPases in the control of tip growth. Plant Cell *9*, 1647–1659.

Lloyd, C., and Hussey, P. (2001). Microtubule-associated proteins in plants—why we need a MAP. Nat. Rev. Mol. Cell Biol. *2*, 40–47.

Mathur, J., Mathur, N., Kernebeck, B., and Hulskamp, M. (2003). Mutations in actin-related proteins 2 and 3 affect cell shape development in *Arabidopsis*. Plant Cell *15*, 1632–1645.

Qiu, J.L., Jilk, R., Marks, M.D., and Szymanski, D.B. (2002). The *Arabidopsis* SPIKE1 gene is required for normal cell shape control and tissue development. Plant Cell *14*, 101–118.

Smith, L.G. (2003). Cytoskeletal control of plant cell shape: getting the fine points. Curr. Opin. Plant Biol. *6*, 63–73.

Ueda, K., Matsuyama, T., and Hashimoto, T. (1999). Visualization of microtubules in living cells of transgenic *Arabidopsis thaliana*. Protoplasma *206*, 201–206.

Wasteneys, G.O., and Galway, M.E. (2003). Remodeling the cytoskeleton for growth and form: an overview with some new views. Annu. Rev. Plant Biol. *54*, 691–722.

Wasteneys, G.O., Willingale-Theune, J., and Menzel, D. (1997). Freeze shattering: a simple and effective method for permeabilizing higher plant cell walls. J. Microsc. *188*, 51–61.

Weigel, D., Ahn, J.H., Blazquez, M.A., Borevitz, J.O., Christensen, S.K., Fankhauser, C., Ferrandiz, C., Kardailsky, I., Malancharuvil, E.J., Neff, M.M., et al. (2000). Activation tagging in *Arabidopsis*. Plant Physiol. *122*, 1003–1013.

Whittington, A.T., Vugrek, O., Wei, K.J., Hasenbein, N.G., Sugimoto, K., Rashbrooke, M.C., and Wasteneys, G.O. (2001). MOR1 is essential for organizing cortical microtubules in plants. Nature *411*, 610–613.

Wittmann, T., Bokoch, G.M., and Waterman-Storer, C.M. (2003). Regulation of leading edge microtubule and actin dynamics downstream of Rac1. J. Cell Biol. *161*, 845–851.

Wu, G., Gu, Y., Li, S., and Yang, Z. (2001). A genome-wide analysis of *Arabidopsis* Rop-interactive CRIB motif-containing proteins that act as Rop GTPase targets. Plant Cell *13*, 2841–2856.

Yang, Z. (2002). Small GTPases: versatile signaling switches in plants. Plant Cell *14*, S375–S388.